Physica **140A** (1986) 142–149
North-Holland, Amsterdam

KINETICS IN CHEMICALLY REACTIVE LIQUIDS

Frank H. STILLINGER
AT & T Bell Laboratories, Murray Hill, NJ 07974, USA

Atomic motions in condensed phases can usefully be described in terms of the geometry of the potential energy hypersurface in multidimensional configuration space. Discrete local minima in this hypersurface generate nonoverlapping basins which span the space. For systems which can undergo chemical reactions, the minima and their basins can be classified according to the numbers of reactant and product species present. Reaction rates are determined by passage over saddle-point regions between contiguous basins with different species populations. These principles are illustrated with molecular dynamics simulation results for molten sulfur, showing how the stable low-temperature medium of octameric rings (S_8) polymerizes and degrades at elevated temperature.

1. Introduction

Chemical reactions arguably constitute the most important class of time-dependent processes that occur in liquids. Understanding them in a general and comprehensive way still remains a major theoretical challenge. The present objective is to show how some recent developments in condensed-phase theory which focus on the differential geometry of potential-energy hypersurfaces[1]) can be adapted naturally and usefully to analyze chemical reactivity in liquids at the atomic level.

Consider a system of N identical atoms, interacting with potential energy $\Phi(\boldsymbol{r}_1, \ldots, \boldsymbol{r}_N)$. We suppose Φ is bounded below, and at least twice differentiable if all pair distances are positive. If wall forces are present to break translational and rotational symmetry, then we can expect Φ to exhibit a discrete set of local minima in the $3N$-dimensional configuration space. Quite general arguments suggest that for large N the number of distinguishable minima (mechanically stable atom arrangements) rises exponentially with N. It makes sense to classify minima on the basis of ϕ, their depth on a per-particle basis ($\phi = \Phi_{\min}/N$), and so we can denote the distribution of minima for large N by $\exp[N\sigma(\phi)]$. The combination $k_B\sigma(\phi)$ is the geometric packing entropy for those stable atomic arrangements with potential $N\phi$.

Each minimum is surrounded by a "basin," defined as the set of configurations $\boldsymbol{r}_1, \ldots, \boldsymbol{r}_N$ which are connected to the minimum by a steepest-descent trajectory

0378-4371/86/$03.50

(tangent to $-\nabla\Phi$) on the Φ hypersurface. Aside from a zero-measure set of boundary points, all configurations can be uniquely assigned in this way to basins. Consequently, essentially any atomic configuration can be resolved into an inherent packing part (the minimum configuration), and a vibrational deformation that displaces the configuration away from the minimum within the same basin.

This separation of inherent packing structure and vibration leads to an exact expression (in the large-N limit) for the classical canonical partition function as a simple quadrature over ϕ:

$$Z_N = \lambda^{-3N} \int \exp\{N[\sigma(\phi) - \beta\phi - \beta f_v(\beta, \phi)]\}\, d\phi. \tag{1.1}$$

Here $\beta = 1/k_B T$ and λ is the thermal deBroglie wavelength. The quantity f_v is the vibrational free energy (per atom) for those minima whose depth is ϕ. Because N is large, the free energy can be obtained simply by evaluating the integrand in eq. (1.1) at its maximum with respect to ϕ. The value $\phi_m(\beta)$ which produces the maximum corresponds to the dominating set of packings for the given temperature. In the case of the thermodynamically stable liquid, these packings are amorphous.

If the system has not achieved equilibrium, eq. (1.1) is not applicable. Nevertheless the exhaustive division of configuration space into basins is a valuable tool for understanding kinetic processes that drive the system eventually to equilibrium.

2. Chemical bonds

For the simple case of liquified noble gases ϕ can be adequately represented by a sum of central pair potentials (such as the Lennard–Jones 12–6 function). However this is not possible in the more interesting cases that involve covalent chemical bond formation. As we shall see below, a combination of two and three-atom potentials qualitatively suffice to represent directional and saturable chemical bonds.

The presence of covalent bonds introduces a distinct separation between chemical and physical length and energy scales. Chemical bonds are much stronger and substantially shorter than those associated with Van der Waals forces. Table I contrasts the mean chemical bond lengths observed in crystals for several elements with the distances to nearest nonbonded neighbors[2]). On account of this separation, there is virtually never any ambiguity about which pairs of atoms are bonded and which are not; and this applies to all packings

TABLE I
Comparison of chemical bond lengths with distances to nearest nonbonded neighbors, in crystals of the elements[a,b]

Element	Mean bond length	Nearest nonbonded neighbor distance
B	1.76	> 2.50
C[c]	1.42	2.46
N	1.06	3.47
O	1.15	3.20
F	1.49	2.82
Si	2.29	3.73
P[d]	2.23	3.59
S	2.06	3.37
Cl	1.98	3.32
As	2.52	3.12
Se	2.37	3.44
Br	2.27	3.32

[a] From Donohue, ref. 2.
[b] All distances in ångstroms.
[c] Graphite.
[d] Black phosphorous.

whether crystalline or not. By introducing a cutoff distance r_c midway between the bonded and nonbonded distances (as those in table I), the criterion

$$r_{ij} \leqslant r_c \tag{2.1}$$

serves to identify all pairs ij which are chemically bonded.

Once pair connections (bonds) have been identified for any stable packing, the corresponding molecular species, the connected atom subsets, can also be identified. By convention we shall suppose that the molecular species identified at the potential minima are applicable throughout the entire respective basins, thereby eliminating ambiguities that might arise from large-amplitude vibrational distortions.

Chemical reaction rates can now be inferred from the manner in which a system, initially localized in a set of basins corresponding to a nonequilibrium population of molecules, spreads outward to equilibrate over the full set of basins.

3. Sulfur model

At low temperatures the stable form of elemental sulfur involves octameric ring molecules (S_8) with each atom chemically bonded to two nearest neighbors.

Without violating the divalency preference, alternative cyclic molecular species S_n can also form, with little change in bond lengths or angles[2]). At high temperatures, these cyclic species can break a bond to form diradical chains, and these chains can link to form high-molecular weight linear polymers. The polymerization process is reversible and cooperative, leading to a distinctive lambda transition in the liquid phase at 159°C[3]).

A combination of atom pair potentials v_2 and atom-triplet potentials v_3 has been identified[4]) which qualitatively reproduces the elaborate structural chemistry of sulfur, and which has permitted molecular dynamics simulations to be carried out for 1000 sulfur atoms. The function v_2 provides for chemical bonds, while v_3 limits them to divalency and enforces the correct bond angle.

Fig. 1 displays an atomic pair correlation function for a liquid at 126°C (melting point is 115°C), consisting entirely of S_8 rings. Vibrational deformation has been removed to enhance the details of short-range order. In other words a representative set of system configurations served as input to steepest descent

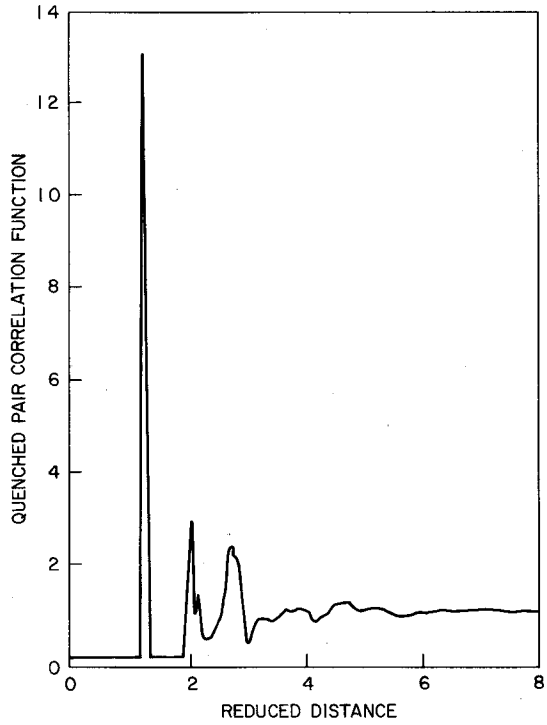

Fig. 1. Quenched pair correlation function corresponding to liquid sulfur (S_8 rings only), at 126°C. All contributing configurations are local potential minima produced by steepest-descent mapping on the potential hypersurface. Distances are measured in units equal to 1.69 Å.

mappings onto potential minima, and fig. 1 shows the pair correlation function averaged over those liquid-phase minima.

The most obvious feature illustrated by fig. 1 is the narrow and isolated peak at reduced distance 1.20. This comprises all bonded pairs (exactly 1000 in this instance). The continuous but structured distribution of other pairs beginning at about reduced distance 1.95 comprises nonbonded intramolecular and intermolecular pairs. Identification of bonds is quite unambiguous in this "quenched" pair correlation function, and the situation is equally unambiguous for quenched pair correlation functions evaluated when other sulfur molecular species (ring and chain) are present.

4. Chemical reactivity and reaction rates

Experimentally, cyclic S_8 molecules remain intact for several hours in the liquid at its melting point. Molecular dynamics simulation in real time proceeds about 10^{15} times more slowly, so no reactivity would be observed at this temperature in a simulation. However the reaction rates can be drastically increased by raising the temperature. In the high temperature regime it is quite feasible to monitor conversion of an initially pure medium of S_8 rings into other species. Following earlier remarks, this is done by extracting a series of system configurations from a high-temperature constant-energy simulation, subjecting each to a steepest-descent quench, and observing what molecular species are present at the corresponding series of potential minima.

Fig. 2 shows how the number of surviving S_8 rings declines with time for two samples suddenly heated from low temperature. Both initially contained 125 S_8 rings. One exhibited mean temperature 870°C during the run, the other 1050°C. Both show reactivity, but temperature dependence of the S_8-ring loss rate is obvious. In both of these runs the density was held fixed at the low-temperature liquid value, 1.805 g/cm^3.

The mean degree of polymerization, on a per-atom basis, is given by

$$d = \sum j^2 n_j / N, \tag{4.1}$$

where n_j is the number of molecular species present containing exactly j sulfur atoms. This quantity is exactly 8 at the beginning of both reaction runs, of course, and then rises as time proceeds. It is gratifying to see that the model agrees with experiment in demonstrating a spontaneous tendency to polymerize at high temperature.

Fig. 3 provides an histogram for the n_j distribution at the end of the 1050°C run. The results are classified also by ring or chain character, the only molecular

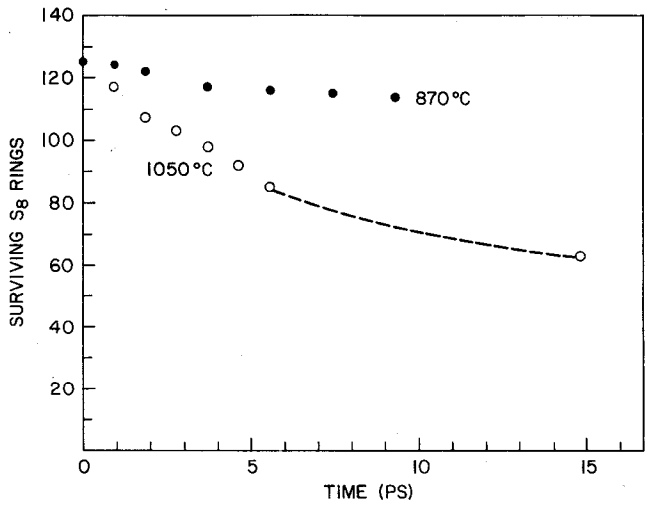

Fig. 2. Time-dependent survival of S_8 rings at elevated temperatures.

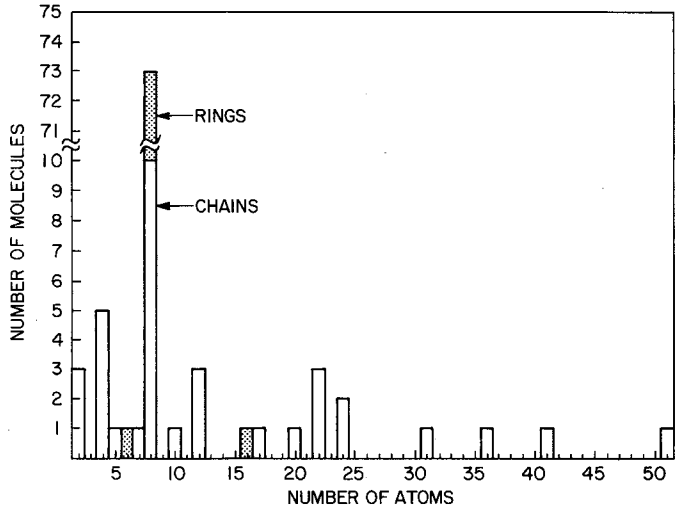

Fig. 3. Populations of ring (dark) and chain (light) species, containing j sulfur atoms, at the end of the 1050°C reaction run.

bonding topologies found to be present. The largest fragment, a diradical S_{51} chain, would be expected to grow further in length if the reaction were allowed to continue. Simultaneous degradation processes have also produced small fragments as well, including sulfur dimers. These degradation-polymerization reactions are endothermic. It is no surprise then to find that in both runs the depths of the potential minima encountered rise as the reaction proceeds.

Since total energy is conserved, and since the reactions are endothermic, kinetic temperature tends to drop slightly during a run. That would be expected to slow reaction rates, but there is a compensating feature that is an important dense medium effect. Diradical chain species produced in the early stages are particularly reactive, with chain ends attacking S_8 rings and breaking them open to form longer chains. A long diradical chain can even coil back on itself and in principal cause its own cleavage. In any case, the reaction becomes autocatalytic after its very early phase.

Initial stages of the reaction, at least for our model, show an unexpected feature. Specifically the n_j distribution is weighted toward even numbers j. For example, even at the end of the lower temperature (870°C) run, no odd-j species were present, even though chains initially formed by ring opening had both polymerized and spontaneously fragmented. In the higher temperature run (1050°C), the first appearance of an odd-j species occurred only after half of the run was completed. Indeed the histogram in fig. 3 for the end of the run shows a continuing bias in favor of even j's.

5. Conclusion

By joining conventional molecular dynamics calculations to steepest-descent mapping onto potential minima, a powerful simulation tool becomes available to study chemical reactions in condensed phases. Normally this will require use of more elaborate potential functions than those composed just of additive atom-pair interactions. But as the sulfur model illustrates, it may often suffice to supplement pair potentials with appropriate three-atom contributions to represent directed and saturable chemical bonds.

It has been shown that a cutoff-distance criterion, eq. (2.1), provides an unambiguous and nonarbitrary means for identifying chemical bonds and hence molecular species, for all potential minima and their respective surrounding basins. In the case of sulfur, it will be desirable in the future to search for the presence of unusual topologies for large ring molecules, namely interlinked rings ("catenane" analogs), and knotted structures (such as the elementary trefoil).

References

1) F.H. Stillinger and T.A. Weber, Science **225** (1985) 983.
2) J. Donohue, The Structures of the Elements (Krieger, Malabar, Florida, 1982).
3) B. Meyer, ed; Elemental Sulfur, Chemistry and Physics (Wiley-Interscience, New York, 1965).
4) F.H. Stillinger, T.A. Weber and R.A. LaViolette, J. Chem. Phys., to be published. F.H. Stillinger and T.A. Weber, J. Chem. Phys., to be published.